

This article was downloaded by: [CDC]

On: 05 July 2012, At: 10:33

Publisher: Taylor & Francis

Informa Ltd Registered in England and Wales Registered Number: 1072954

Registered office: Mortimer House, 37-41 Mortimer Street, London W1T 3JH, UK



## Aerosol Science and Technology

Publication details, including instructions for authors and subscription information:

<http://www.tandfonline.com/loi/uast20>

### A Simplified Model of Interceptional Deposition of Fibers at Airway Bifurcations

B. Asgharian<sup>a</sup> & C. P. Yu<sup>a</sup>

<sup>a</sup> Department of Mechanical and Aerospace Engineering, State University of New York at Buffalo, Amherst, NY, 14260

Version of record first published: 07 Jun 2007

To cite this article: B. Asgharian & C. P. Yu (1989): A Simplified Model of Interceptional Deposition of Fibers at Airway Bifurcations, *Aerosol Science and Technology*, 11:1, 80-88

To link to this article: <http://dx.doi.org/10.1080/02786828908959301>

PLEASE SCROLL DOWN FOR ARTICLE

Full terms and conditions of use: <http://www.tandfonline.com/page/terms-and-conditions>

This article may be used for research, teaching, and private study purposes. Any substantial or systematic reproduction, redistribution, reselling, loan, sub-licensing, systematic supply, or distribution in any form to anyone is expressly forbidden.

The publisher does not give any warranty express or implied or make any representation that the contents will be complete or accurate or up to date. The accuracy of any instructions, formulae, and drug doses should be independently verified with primary sources. The publisher shall not be liable for any loss, actions, claims, proceedings, demand, or costs or damages whatsoever or howsoever caused arising directly or indirectly in connection with or arising out of the use of this material.

# A Simplified Model of Interceptional Deposition of Fibers at Airway Bifurcations

B. Asgharian and C. P. Yu

*Department of Mechanical and Aerospace Engineering, State University of New York at Buffalo, Amherst, NY 14260*

Based on a simplified model, a theoretical expression for the deposition efficiency of fibers by interception at the bifurcation of a parent-daughter system was derived. In deriving this expression, the simultaneous effect of the velocity shear of the flow and Brownian rotation on fiber orientation was considered. Calculated deposition effi-

ciencies in different airway generations of a Weibel lung model showed that the results obtained previously by Harris and Frazer in 1976 were valid only for small fibers. More accurate deposition results for large fibers are presented in this paper.

## INTRODUCTION

At the bifurcation site of an airway in the lung, inhaled fibers can be deposited by the combined mechanisms of impaction and interception. If the branching angle at the bifurcation is small and the flow velocity is low, impaction becomes less important and the site of deposition reduces to a single line which bisects the airway cross section at the exit of the parent tube. This simplified geometrical model was first formulated by Harris and Fraser (1976) to estimate the interceptional deposition of fibers at an airway bifurcation in the human lung.

In a shear flow, it is known that fibers are subjected to a combined translational and rotational motion. The fiber orientation, as a result of the rotational motion, is controlled by the velocity shear in the flow as well as by Brownian motion which arises from the bombardment of air molecules. Both fiber length and orientation are the particle factors that determine the amount of deposition at a bifurcation by interception. In their analysis, Harris and Fraser assumed that fibers were in pure periodic rotation in the shear flow when the root mean square of the Brownian rotation angle was less than  $10^\circ$ ,

and beyond that point fibers were oriented randomly. This assumption introduced a discontinuity in deposition efficiency, leading to physically inconsistent results.

In this paper, the problem of Harris and Fraser is reexamined despite its oversimplified geometry. An approximate solution is found which allows a smooth transition of the efficiency from the velocity dominated rotation to the one controlled by Brownian motion. Interceptional deposition in different generations of a Weibel lung model (1963) is then calculated for various fiber sizes and compared with the results of Harris and Fraser.

## DEPOSITION EFFICIENCY

At any time  $t$ , the orientation of fibers, expressed by an orientation distribution function  $P(\phi, \theta, t)$  is governed by the Fokker-Planck equation (Peterlin, 1938)

$$\frac{\partial P}{\partial t} + \nabla \cdot (\bar{\omega}P - 'D\nabla P) = 0, \quad (1)$$

where  $\omega$  is the angular velocity of the particle,  $'D$  is the Brownian diffusion coefficient for rotation, and  $\phi$  and  $\theta$  are the Eulerian angles shown in Figure 1. The solution of  $P$

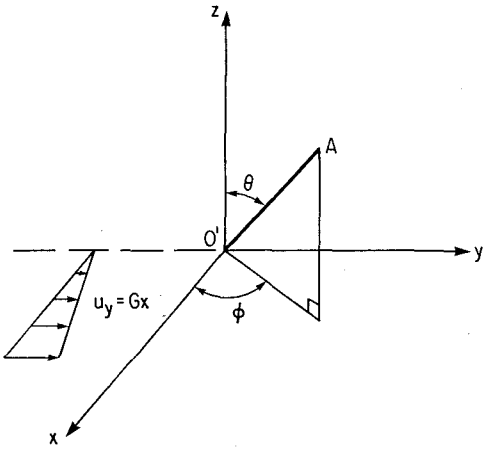


FIGURE 1. Orientation of a fiber.

must satisfy the condition

$$\int_0^{2\pi} \int_0^{\pi/2} P(\phi, \theta, t) \sin \theta \, d\theta \, d\phi = 1. \quad (2)$$

The interceptional deposition of fibers at the bifurcation of a parent-daughter airway system can be derived from pure geometrical considerations as follows: we consider a parent airway of radius  $R$  and length  $L$  in which a fibrous aerosol of uniform concen-

tration flows downstream with a parabolic velocity (Figure 2). A bifurcation line  $HH'$  bisecting the airway cross-sectional area is located at the end of the airway. Let  $O'A$  represent the fiber half-length  $l_f/2$  with  $O'$  at the midpoint of the fiber. A coordinate system  $xyz$  is placed at  $O'$  such that the  $x$  axis is in the radial direction of the airway cross section or the direction of the velocity gradient, and the  $y$  axis points the flow direction. Accordingly, the  $z$  axis which lies in the cross-sectional plane of the airway is tangential to the circle of radius  $\overline{OO'}$ , where  $O$  is on the axis of the airway. From Figure 2, the projection of the fiber half-length  $l_p/2$  on the cross-sectional plane of the airway,  $\overline{O'B}$ , is

$$\overline{O'B} = (\overline{O'E}^2 + \overline{O'D}^2)^{1/2}, \quad (3)$$

where  $\overline{O'E}$  and  $\overline{O'D}$  are, respectively, the components of  $\overline{O'A}$  in the  $x$  and  $z$  directions, given by

$$\overline{O'E} = \overline{O'A} \cos \theta = \frac{l_f}{2} \cos \theta, \quad (4)$$

and

$$\overline{O'D} = \overline{O'C} \cos \phi = \frac{l_f}{2} \sin \theta \cos \phi. \quad (5)$$

Thus,

$$\overline{O'B} = \left( \frac{l_f^2}{4} \sin^2 \theta \cos^2 \phi + \frac{l_f^2}{4} \cos^2 \theta \right)^{1/2}, \quad (6)$$

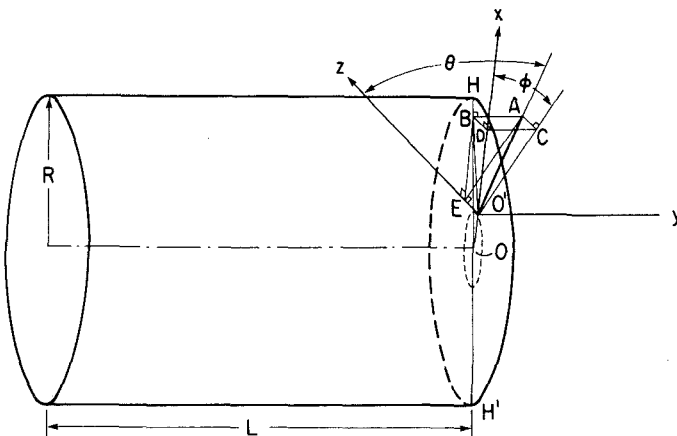


FIGURE 2. Geometrical description of a fiber in a parent airway for the analysis of interceptional deposition.

or

$$l_p = l_f (1 - \sin^2 \theta \sin^2 \phi)^{1/2}. \quad (7)$$

To determine deposition efficiency by interception at the bifurcation, we examine a quadrant of the cross section shown in Figure 3. Interceptional deposition occurs when the fiber projection intercepts the bifurcation line  $\overline{OH}$ ; the limiting case of which is when one end of the projection is on  $\overline{OH}$ . At this limit, the midpoint of the projected length  $O'$  describes a curve  $OO'$ , shown by the dashed line, such that all the fibers with their midpoints traveling between this line and the bifurcation line  $\overline{OH}$  are captured. The interceptional deposition efficiency is the fraction of fibers in the airway passing through this region, and is defined as the volume flow rate through this region divided by the flow rate through one quadrant of the airway cross section. To derive a mathematical expression for the interceptional deposition efficiency, we first consider Figure 3a. From the law of cosines, we find angle  $\Omega$  in triangle  $O'BK$  to be:

$$\Omega = \cos^{-1} \left( \frac{l_f \cos \theta}{l_p} \right). \quad (8)$$

Next, we consider triangle  $K'O'B$ . Angle  $K'\hat{O}'K$  in this triangle is equal to  $\pi/2 - \Gamma$ . Also, in triangle  $K'O'B$ , angle  $K'\hat{B}O'$  is  $\Gamma - \Omega$ . Thus, from triangle  $OO'B$ , we obtain

from the law of sines the following relations:

$$\frac{\sin\left(\frac{\pi}{2} - \Gamma\right)}{l_p/2} = \frac{\sin(\Gamma - \Omega)}{r}, \quad (9)$$

or

$$r = \frac{l_p \sin(\Gamma - \Omega)}{2 \cos \Gamma}, \quad (10)$$

where  $r = \overline{OO'}$  is the radial position of the midpoint of the fiber. Figure 3b shows the position when  $B$  coincides with  $H$ . At this position, one finds from triangle  $OO'H$  the following additional relations:

$$\frac{R}{\sin\left(\Omega + \frac{\pi}{2}\right)} = \frac{l_p/2}{\sin\left(\frac{\pi}{2} - \Gamma'\right)}, \quad (11)$$

$$\cos \Gamma' = \frac{l_p}{2R} \cos \Omega, \quad (12)$$

$$\Gamma' = \cos^{-1} \left( \frac{l_p}{2R} \cos \Omega \right), \quad (13)$$

and

$$r = r' = \frac{l_p \sin(\Gamma' - \Omega)}{2 \cos \Gamma'}. \quad (14)$$

Consider a differential area  $dA$  in Figure 3b. The flow in this area is  $q = udA$  where  $u$  is the local velocity of the flow. The fraction of fibers in the airway,  $dI$ , with Eulerian

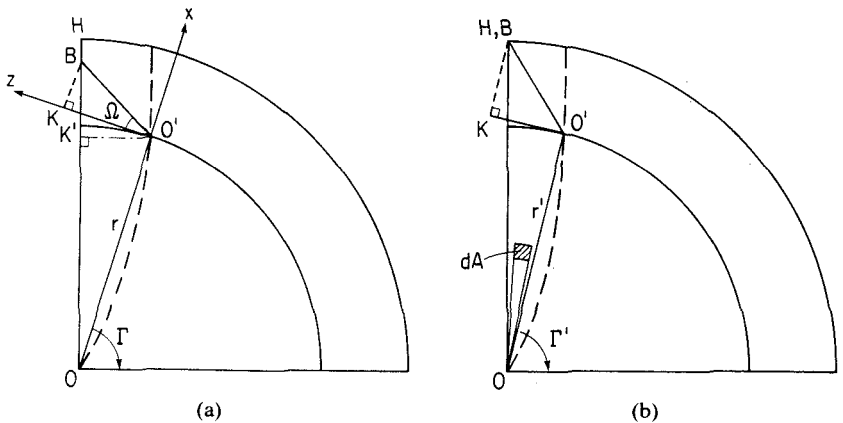


**FIGURE 3.** Interception of a fiber in a quadrant of cross section at the bifurcation. (a) The end of the fiber in contact with an arbitrary point on the bifurcation line. (b) The end of the fiber is in contact with  $H$ .

angles  $\phi$  and  $\theta$  whose midpoints are inside the differential area is

$$dI = \frac{P(r, \phi, \theta) \sin \theta u dA}{Q}, \quad (15)$$

where  $Q$  is the flow through one quadrant of the cross section of the airway, and  $P(r, \phi, \theta)$  is the orientation distribution function obtained from Eq. (1). The interceptional deposition efficiency is then

$$\begin{aligned} I(\phi, \theta) &= \frac{8 \sin \theta}{\pi R^4} \iint_A P(r, \phi, \theta) r (R^2 - r^2) dr d\Gamma \\ &= \frac{8 \sin \theta}{\pi} \\ &\quad \times \left\{ \int_{\Gamma=0}^{\Gamma'} \int_{r^*=0}^{(l_p/2)(\sin(\Gamma-\Omega)/\cos \Gamma)} \right. \\ &\quad \times P(r^*, \phi, \theta) r^* (1 - r^{*2}) dr^* d\Gamma \\ &\quad \left. + \int_{\Gamma=\Gamma'}^{\pi/2} \int_{r^*=0}^{r^{**}} P(r^*, \phi, \theta) \right. \\ &\quad \left. \times r^* (1 - r^{*2}) dr^* d\Gamma \right\}, \quad (16) \end{aligned}$$

where  $r^* = r/R$  and  $l_p^* = l_p/R$ . Integrating Eq. (16) over all Eulerian angles gives the total efficiency by interception as

$$\eta = \int_{\phi=0}^{2\pi} \int_{\theta=0}^{\pi/2} I(\phi, \theta) d\theta d\phi. \quad (17)$$

To evaluate Eqs. (16) and (17), we need to find an expression for  $P(r^*, \phi, \theta)$ . Peterlin (1938) studied the orientation of suspended ellipsoidal particles in a constant shear flow. He solved the Fokker-Planck Eq. (1) to obtain a steady-state solution in the form:

$$\begin{aligned} P(\phi, \theta) &= \frac{1}{2\pi} \left\{ 1 + \frac{3\Delta \sin^2 \theta}{1 + \left(\frac{6}{rPe}\right)^2} \left( -\frac{1}{2} \cos 2\phi + \frac{3}{rPe} \sin 2\phi \right) + \frac{\Delta^2}{1 + \left(\frac{6}{rPe}\right)^2} \right. \\ &\quad \times \left[ -\frac{3}{14} (3 \cos^3 \theta - 1) + \frac{9}{560} (35 \cos^4 \theta - 30 \cos \theta + 3) + \frac{15 \sin^4 \theta}{16 \left(1 + \frac{100}{rPe^2}\right)} \right. \\ &\quad \left. \left. \times \left( \cos 4\phi \left(1 - \frac{60}{rPe^2}\right) - \frac{16}{rPe} \sin 4\phi \right) \right] + \Delta^3 [\dots] \right\}, \quad (18) \end{aligned}$$

where

$$\Delta = \frac{\beta^2 - 1}{\beta^2 + 1}, \quad (19)$$

$\beta$  is the aspect ratio of the fiber, and  $rPe$  is the rotational Peclet number, defined by

$$rPe = \frac{G}{rD}, \quad (20)$$

in which  $G$  is the velocity gradient, and  $rD$  is the rotational diffusion coefficient, given by

$$rD = B_\omega kT. \quad (21)$$

In Eq. (21),  $B_\omega$  is the angular mobility of the fiber,  $k$  is the Boltzmann constant, and  $T$  is the absolute temperature. For a prolate ellipsoid of revolution, it was found that (Gans, 1928)

$$B_\omega = \frac{3 \left[ \frac{2\beta^2 - 1}{\sqrt{\beta^2 - 1}} \ln(\beta + \sqrt{\beta^2 - 1}) - \beta \right]}{2\pi\mu d_f^3 (\beta^4 - 1)}, \quad (22)$$

where  $d_f$  is the particle minor diameter.

Equation (18) reduces to the following simple forms when  $rPe$  approaches zero and infinity, which correspond, respectively, to the cases of very strong and weak Brownian rotation:

$$P(\phi, \theta) = \frac{1}{2\pi}, \quad (23)$$

and

$$P(\phi, \theta) = \frac{1}{2\pi} \left\{ 1 - \frac{3\Delta}{2} \cos 2\phi \sin^2 \theta + \Delta^2 \right. \\ \times \left[ \frac{3}{80} (15 \cos^4 \theta - 30 \cos^2 \theta + 7) \right. \\ \left. \left. + \frac{15}{16} \cos 4\phi \sin^4 \theta \right] - \Delta^3 [\dots] \right\}. \quad (24)$$

Equation (18) can be applied locally to a parabolic flow in a circular tube where the velocity gradient is a function of the radial position. Since Eq. (18) is a series solution of  $\Delta$ , a rapid convergence of this equation requires  $\Delta \ll 1$ , which corresponds to small values of  $\beta$ . However, for fibers with large  $\beta$ ,  $\Delta$  approaches unity and a large number of terms in Eq. (18) is needed for an accurate result.

#### APPROXIMATE SOLUTION

For strong Brownian rotation, Eq. (16) becomes

$$I(\phi, \theta) = \frac{8 \sin \theta}{\pi R^4} \iint_A \left( \frac{1}{2\pi} \right) r (R^2 - r^2) dr d\Gamma \\ = I_R(\phi, \theta). \quad (25)$$

Carrying out the integration, we obtain

$$I_R(\phi, \theta) = \frac{2 \sin \theta}{\pi^2} \left\{ \left( \frac{l_p^*}{2} \right)^2 \left[ \cos^2 \Omega (\tan \Gamma' - \Gamma') - \sin 2\Omega (\ln \sec \Gamma') + \Gamma' \sin^2 \Omega \right] - \frac{1}{2} \left( \frac{l_p^*}{2} \right)^4 \right. \\ \times \left[ \cos^4 \Omega \left( \frac{\tan^3 \Gamma'}{3} - \tan \Gamma' + \Gamma' \right) - 4 \cos^3 \Omega \sin \Omega \left( \frac{\tan^2 \Gamma'}{2} - \ln \sec \Gamma' \right) \right. \\ \left. \left. + \frac{3}{2} \sin^2 2\Omega (\tan \Gamma' - \Gamma') - 4 \cos \Omega \sin^3 \Omega (\ln \sec \Gamma') + \Gamma' \sin^4 \Omega \right] \right. \\ \left. + \left( r^{*/2} - \frac{r^{*/4}}{2} \right) \left( \frac{\pi}{2} - \Gamma' \right) \right\}. \quad (26)$$

The total efficiency for the random fiber orientation is

$$\eta_R = \int_{\phi=0}^{2\pi} \int_{\theta=0}^{\pi/2} I_R(\phi, \theta) d\theta d\phi. \quad (27)$$

When the fiber is sufficiently large, its orientation is controlled by the velocity shear. Jeffery (1922) obtained the following results for the Eulerian angles:

$$\tan \phi = \beta \tan \left( \frac{2\pi t}{\tau} + C_1 \right), \quad (28)$$

and

$$\tan \theta = \frac{C_2}{(\beta^2 \cos^2 \phi + \sin^2 \phi)^{1/2}}, \quad (29)$$

where  $t$  is the elapsed time and  $\tau$  is the period of rotation, given by

$$\tau = \frac{2\pi(l_f^2 + d_f^2)}{l_f d_f G}, \quad (30)$$

and  $C_1$  and  $C_2$  are constants related to the initial Eulerian angles  $\phi_0, \theta_0$  by

$$C_1 = \tan^{-1} \left( \frac{\tan \phi_0}{\beta} \right), \quad (31)$$

and

$$C_2 = \tan \theta_0 (\beta^2 \cos^2 \phi_0 + \sin^2 \phi_0)^{1/2}. \quad (32)$$

It is apparent from the above results that interceptional deposition depends on the initial orientation of fibers. Thus, for a parabolic flow at the exit of the parent tube, we

may write for the velocity-shear controlled rotation,

$$\begin{aligned}
 I(\phi, \theta) &= \frac{8 \sin \theta}{\pi R^4} \iint_A P(r, \phi, \theta) r (R^2 - r^2) dr d\Gamma \\
 &= I_P(\phi_0, \theta_0), \tag{33}
 \end{aligned}$$

since  $\phi$  and  $\theta$  in  $P(r, \phi, \theta)\sin\theta$  are functions of  $\phi_0, \theta_0$ , and the residence time of the fibers in the airway. The total interceptional deposition efficiency for all Eulerian angles is

$$\eta_P = \int_{\phi_0=0}^{2\pi} \int_{\theta_0=0}^{\pi/2} I_P(\phi_0, \theta_0) d\theta_0 d\phi_0. \tag{34}$$

The values of  $\eta_P$  can be computed numerically using Eq. (28) and (29) for a given initial orientation. Equations (33) and (34) also apply to other flow fields if a substitution for the velocity profile is made in Eq. (33).

We assume an approximate solution of Eq. (17) in the form of a linear combination as

$$\eta = f_1('Pe) \eta_P + f_2('Pe) \eta_R, \tag{35}$$

where the weighting functions  $f_1$  and  $f_2$  are assumed to have the form

$$f_1 = \frac{('Pe)^b}{a + ('Pe)^b}, \tag{36}$$

and

$$f_2 = \frac{a}{a + ('Pe)^b}, \tag{37}$$

In Eq. (35)  $'Pe$  is the rotational Peclet number defined by Eq. (20) with  $G = U/R$ , where  $U$  is the average velocity of the flow and  $a$  and  $b$  are constants to be determined by matching the approximate solution (35) with Eq. (17).

**DETERMINATION OF  $a$  AND  $b$**

To determine constants  $a$  and  $b$ , we used the series solution of  $P(\phi, \theta)$  given by Eqs. (18), (23), and (24) and substituted them into

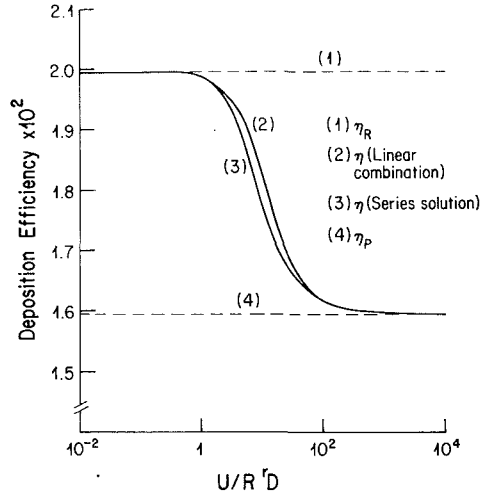


**FIGURE 4.** Comparison of  $\eta$  calculated from the exact series solution (17) and from the linear combination solution (35).

Eq. (17) for computation of  $\eta, \eta_R$ , and  $\eta_P$ . For all values of  $'Pe$ , it was found that  $a = 50$  and  $b = 1.5$  provided an excellent matching for the value of  $\eta$  calculated from Eq. (35) and those from Eq. (17). The values of  $a$  and  $b$  were found to be insensitive to  $\beta$ . Figure 4 shows a comparison of  $\eta$  for  $\beta = 50$  determined from various formulas for the flow condition equivalent to the 15th airway generation of the Weibel lung model (1963). The difference in  $\eta$  between the exact series solution (17) and the linear combination solution (35) is less than 6%. Figure 4 also shows that the velocity shear effect on fiber rotation becomes important when  $'Pe$  exceeds 0.01, and when  $'Pe$  is greater than  $10^3$ , the rotation of fiber is completely controlled by the shear flow.

**DEPOSITION IN AIRWAYS**

Interceptional deposition efficiency as a function of the aspect ratio of the fiber is calculated using Eq. (35) in which  $\eta_R$  and  $\eta_P$  are determined respectively from Eqs. (27) and (34). The results for a fiber diameter of  $0.3 \mu\text{m}$  at a flow rate of  $375 \text{ cm}^3/\text{s}$  in the

Downloaded by [CDC] at 10:33 05 July 2012

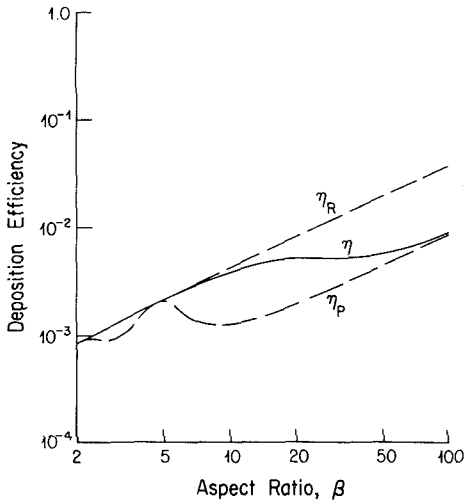


**FIGURE 5.** Deposition efficiency by interception as a function of  $\beta$  at  $d_f = 0.3 \mu\text{m}$  and a flow rate of  $375 \text{ cm}^3/\text{s}$  in the 15th airway generation of Weibel's lung model.

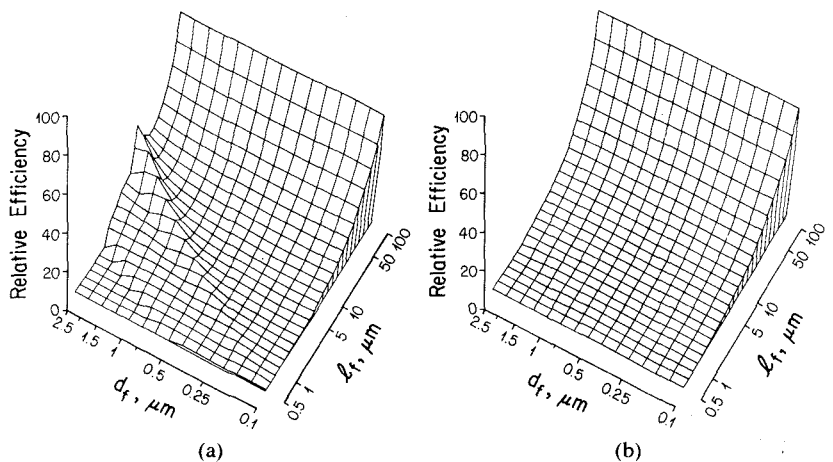
15th generation of the airways of Weibel's lung model are depicted in Figure 5. Again, in this figure, curve 1 represents the periodic rotation solution  $\eta_P$  given by Eq. (34), and curve 3 corresponds to the random orientation solution  $\eta_R$  calculated from Eq. (27). As  $\beta$  increases,  $\eta_R$  increases monotonically while  $\eta_P$  shows an oscillatory variation pattern with  $\beta$  for  $\beta < 10$ , caused by large variations in fiber orientation at the bifurcation.

Since fibers controlled by the shear flow tend to align themselves to the flow,  $\eta_P$  is found to be always smaller than  $\eta_R$ . The linear combination solution (35) shown by curve 2 gives the same results of  $\eta_R$  for small  $\beta$  and it approaches the value of  $\eta_P$  for large  $\beta$ .

Figure 6 presents the variations of  $\eta_R$  and  $\eta_P$  with both fiber length and diameter in the 15th airway generation of Weibel's lung model at a flow rate of  $375 \text{ cm}^3/\text{s}$ . The periodic rotation solution  $\eta_P$  shown in Figure 6a depends upon both fiber length and diameter, while the random orientation solution  $\eta_R$  shown in Figure 6b depends solely on the fiber length.

The interceptional deposition efficiency beyond the fifth airway generation of Weibel's lung model calculated from Eq. (35) is compared with the results of Harris and Fraser (1976) in Figure 7 for several fiber equivalent volume diameters  $d_{ev}$  ( $d_{ev} = d_f \beta^{1/3}$ ) at  $\beta = 10$ . The velocity profile at the exit of each airway generation is assumed to be parabolic. For small  $d_{ev}$  for which Brownian rotation controls the fiber orientation, two results are almost identical. However, as  $d_{ev}$  increases the periodic rotation becomes in-

**FIGURE 6.** Relative deposition efficiency by interception as a function of fiber size in the 15th airway generation of Weibel's lung model at a flow rate of  $375 \text{ cm}^3/\text{s}$ . (a)  $\eta_P$ ; (b)  $\eta_R$ .





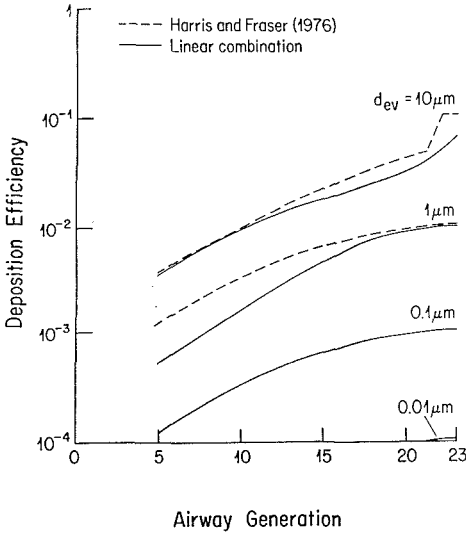


**FIGURE 7.** Deposition efficiency by interception in different airway generations of Weibel's lung model at a flow rate of  $375 \text{ cm}^3/\text{s}$  for  $\beta = 10$ . Dotted lines are the results by Harris and Fraser (1976) and solid lines are the results calculated from Eq. (35).

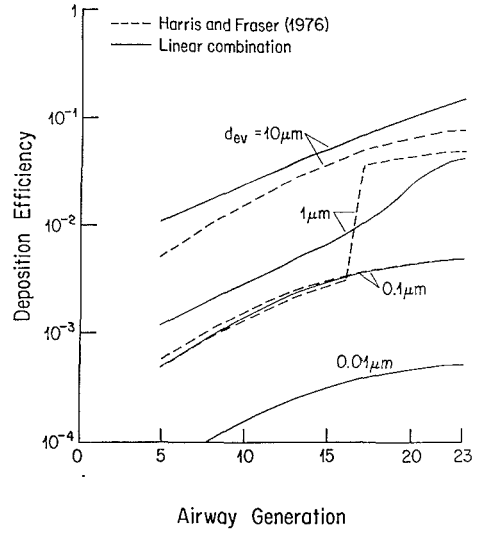
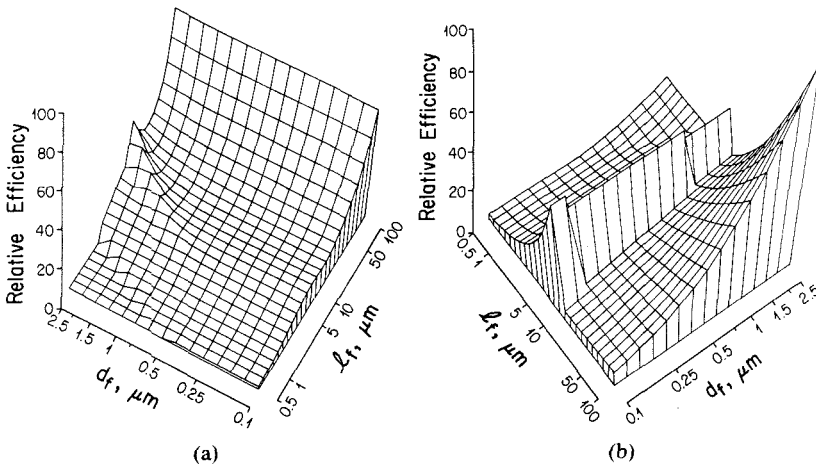


**FIGURE 8.** Deposition efficiency by interception in different airway generations of Weibel's lung model at a flow rate of  $375 \text{ cm}^3/\text{s}$  for  $\beta = 100$ . Dotted lines are the results by Harris and Fraser (1976) and solid lines are the results calculated from Eq. (35).

creasingly important, the formulas derived by Harris and Fraser show a discontinuity in deposition because of the sudden switching from a random orientation to a velocity shear controlled orientation. Figure 8 shows the comparison of our results with those of Harris and Fraser for  $\beta = 100$ . Harris and

**FIGURE 9.** Relative deposition efficiency by interception as a function of fiber size in the 15th airway generation of Weibel's lung model at a flow rate of  $375 \text{ cm}^3/\text{s}$ . (a) Equation (35); (b) Harris and Fraser (1976).



Fraser predicted a smaller deposition for fibers with  $d_{ev} = 1 \mu\text{m}$ . This is obviously unreasonable because it implies that long fibers have a lower interceptional deposition than the short ones.

A different representation of the comparison between the results from Eq. (35) with that of Harris and Fraser is shown in Figure 9, in which interceptional deposition efficiency in the 15th airway generation of Weibel's lung model is plotted versus both fiber length and diameter at a flow rate of  $375 \text{ cm}^3/\text{s}$ . Except for the oscillatory variation pattern at small  $\beta$ , the deposition results calculated from Eq. (35) are always found to increase with the fiber length, as shown in Figure 9a. The results of Harris and Fraser shown in Figure 9b, however, have several discontinuities. The variations

of deposition with fiber diameter and length predicted by their formulas do not appear to be justified from physical grounds.

---

This research was supported by grant HL 38503 from the National Institutes of Health.

---

## REFERENCES

- Gans, K. R. (1928). *Ann. Phys.* 86:628-656.
- Harris, R. L., and Fraser, D. A. (1976). *Am. Ind. Hyg. Assoc. J.* 37:73-89.
- Jeffery, G. B. (1922). *Proc. R. Soc. Lond.* A102:161-179.
- Peterlin, A. (1938). *Z. Phys.* 111:232-263.
- Weibel, E. R. (1963). *Morphometry of the Human Lung*. Academic Press, New York.

Received 10 February 1988; accepted 27 May 1988